Low-energy elastic scattering of electrons by ethylene

L. M. Brescansin
Instituto de Física, UNICAMP, 13083-970 Campinas, São Paulo, Brazil

L. E. Machado
Departamento de Física, UFSCar, 13565-905 São Carlos, São Paulo, Brazil

M.-T. Lee
Departamento de Química, UFSCar, 13565-905 São Carlos, São Paulo, Brazil

(Received 16 September 1997; revised manuscript received 16 December 1997)

Elastic differential, integral, and momentum-transfer cross sections are reported for electron scattering by C_2H_4 at impact energies ranging from 1 to 50 eV. The Schwinger iterative variational method in the fixed-nuclei, static-exchange plus correlation-polarization approximation is used to calculate the scattering amplitudes. Integrated cross sections are also calculated below 1 eV, showing the existence of a Ramsauer-Townsend minimum in this region. Our calculated cross sections are compared with recent experimental data and other theoretical results. [S1050-2947(98)00405-3]

PACS number(s): 34.80.Bm

I. INTRODUCTION

Elastic scattering of low-energy electrons from small polyatomic molecules has been a subject of increasing interest both theoretically and experimentally. The study of scattering properties is of great practical importance in a variety of plasma phenomena (etching, chemical vapor deposition, etc.) and in the understanding of the physics and chemistry of planetary atmospheres and interstellar media.

Although hydrocarbons constitute an important group of such molecules, among them only methane has received a considerable degree of attention in the past few years. For ethylene, although a few recent experimental data on elastic scattering are now available, much less attention has been devoted as yet. In 1985, Floeder *et al.* [1] measured total cross sections for ethylene between 5 and 400 eV in a transmission experiment. In 1986, Sueoka and Mori [2] reported total cross sections for C_2H_4 and C_2H_6 in the (1–400)-eV range, measured using a retarding potential time-of-flight method. In 1992, Mapstone and Newell [3] reported measurements for elastic differential cross sections (DCSs) for e^--C_2H_4 for electron energies of 3–15 eV and for scattering angles of 30°–140°. Finally, Lunt *et al.* [4] studied low-energy elastic e^--C_2H_4 scattering using two different synchrotron radiation photoionization spectrometers, focusing attention in the energy range below 2 eV. From the theoretical point of view, the studies on e^--C_2H_4 elastic scattering have been more sparse. To our knowledge, only two calculations on this molecule have so far been reported in the literature: Schneider *et al.* [5] used the complex Kohn variational method to calculate partial integrated cross sections ($^2B_{2g}$ and ^2A_g symmetries) below 5.5 eV and Winstead *et al.* [6] reported elastic DCSs, calculated within the static-exchange (SE) approximation, from 5 to 20 eV using the Schwinger multichannel method.

In this work we report calculated (DCSs), integral cross sections (ICSs), as well as momentum-transfer cross sections (MTCSs) for elastic scattering of electrons by C_2H_4 for incident energies ranging from 1 to 50 eV. Our description of the electron-molecule collision goes beyond the SE approximation through the inclusion of a scattering-electron correlation as well as polarization of the target electron cloud. It is known [5] that an adequate theoretical description of low-energy electron collisions with atoms or molecules requires a proper balance of the direct electrostatic interaction, the electron exchange, and the electron correlation. Yet the inclusion of polarization effects and target distortion has been shown to produce elastic cross sections qualitatively different from the SE value at low energies [7]. Our scattering amplitudes are calculated using the Schwinger variational iterative method (SVIM) [8,9], a tool capable of providing highly converged estimates of the partial-wave T-matrix elements and scattering wave functions. This method has been recently applied to study photoionization cross sections and elastic scattering of electrons by nonlinear molecules [10–12]. Recently, the SVIM codes were extended in order to permit the inclusion of the correlation-polarization contribution to the electron-molecule interaction potential. Such a contribution was taken into account by following the prescription given by Padial and Norcross [13]. To our knowledge, no theoretical DCSs including correlation-polarization effects have yet been published for ethylene.

The organization of this paper is the following. In Sec. II the theory is briefly described and some details of the calculations are given. Our calculated results and discussions are presented in Sec. III. Section IV summarizes our conclusions.

II. THEORY AND CALCULATION

The Schrödinger equation for the continuum scattering orbitals can be written (in atomic units) as

$$[-\nabla^2 + U(\vec{r}) - k^2]\Psi_{\vec{k}}(\vec{r}) = 0, \tag{1}$$

where $U(\vec{r}) = 2V(\vec{r})$ and $V(\vec{r})$ is the interaction potential

TABLE I. Cartesian Gaussian functions used in the SCF calculations. Cartesian Gaussian basis functions are defined as $\phi^{\alpha,\ell,m,n,\mathbf{A}}(\mathbf{r})=N(x-\mathbf{A}_x)^{\ell}(y-\mathbf{A}_y)^{m}(z-\mathbf{A}_z)^{n}\exp(-\alpha|\mathbf{r}-\mathbf{A}|^2)$, with N a normalization constant.

	d		p		d	
Atom	Exponent	Coefficient	Exponent	Coefficient	Exponent	Coefficient
C	4232.61	0.006228	18.1557	0.039196		
	634.882	0.047676	3.98640	0.244144		
	146.097	0.231439	1.14290	0.816775		
	42.4974	0.789108				
	14.1892	0.791751				
	1.96660	0.321870				
	5.14770	1.000000	0.35940	1.000000	1.500	1.000000
	0.49620	1.000000	0.11460	1.000000	0.750	1.000000
	0.15330	1.000000	0.04584	1.000000	0.300	1.000000
	0.06132	1.000000	0.02000	1.000000		
C*M*	0.03000	1.000000	0.00500	1.000000	0.085	1.000000
	0.01000	1.000000				
	0.00300	1.000000				
H	33.6444	1.000000	1.00000	1.000000		
	5.05796	1.000000	0.50000	1.000000		
	1.14680	1.000000	0.10000	1.000000		
	0.321144	1.000000				
	0.101309	1.000000				

between the target and the scattering electron. Equation (1) can be converted into an equivalent Lippmann-Schwinger equation

$$\Psi_{\vec{k}}^{(\pm)}=\Phi_{\vec{k}}+G_0^{(\pm)}U\Psi_{\vec{k}}^{(\pm)}, \tag{2}$$

with $G_0^{(\pm)}$ being the free-particle Green's operator with outgoing- ($G_0^{(+)}$) or incoming-wave ($G_0^{(-)}$) boundary conditions. In order to take advantage of the symmetry of the target, the scattering wave functions can be partial-wave expanded as

$$\Psi_{\vec{k}}^{(\pm)}(\vec{r})=\left[\frac{2}{\pi}\right]^{1/2}\frac{1}{k}\sum_{p,\mu,l,h} i^l\Psi_{k,lh}^{(\pm)p\mu}(\vec{r})X_{lh}^{p\mu}(\hat{k}), \tag{3}$$

where $X_{lh}^{p\mu}(\hat{r})$ are generalized spherical harmonics, related to the usual spherical harmonics Y_{lm} by

$$X_{lh}^{p\mu}(\hat{r})=\sum_m b_{lhm}^{p\mu}Y_{lm}(\hat{r}). \tag{4}$$

Here p is an irreducible representation (IR) of the molecular point group, μ is a component of this representation, and h distinguishes between different bases of the same IR corresponding to the same value of l. The coefficients $b_{lhm}^{p\mu}$ satisfy important orthogonality conditions and are tabulated for the C_{2v} and O_h groups by Burke *et al.* [14]. The Schwinger variational expression for the T matrix can be written in the bilinear form as

$$T_{\vec{k},\vec{k}_0}^{(\pm)}=\langle\Phi_{\vec{k}}^{(\mp)}|U|\tilde{\Psi}_{\vec{k}_0}^{(\pm)}\rangle+\langle\tilde{\Psi}_{\vec{k}}^{(\mp)}|U|\Phi_{\vec{k}_0}^{(\pm)}\rangle -\langle\tilde{\Psi}_{\vec{k}}^{(\mp)}|U-UG_0^{(\pm)}U|\tilde{\Psi}_{\vec{k}_0}^{(\pm)}\rangle, \tag{5}$$

with $\tilde{\Psi}_{\vec{k}}^{(\pm)}$ denoting trial scattering wave functions. Using partial-wave expansions similar to Eq. (3) for both $\tilde{\Psi}_{\vec{k}}^{(\pm)}$ and

TABLE II. Basis set used for the initial scattering functions.

Scattering symmetry	Center	Gaussian function	Exponents
ka_1	C	s	2.0, 0.5, 0.1, 0.02
		z	4.0, 1.0, 0.25, 0.05
		x^2,y^2,z^2	0.2, 0.05
	c.m.	s	2.0, 0.5, 0.1, 0.02
		z	2.0, 0.5, 0.1, 0.02
		x^2,y^2,z^2	0.2, 0.05
	H	s	1.0, 0.2, 0.05
		x,z	1.0, 0.2, 0.05
ka_2	C	xy	1.0, 0.2, 0.04
	c.m.	xy	0.1, 0.02
	H	y	1.0, 0.2, 0.04
kb_1	C	y	2.0, 0.5, 0.1, 0.02
	c.m.	y	2.0, 0.5, 0.1, 0.02
		yz	0.1, 0.02
	H	y	1.0, 0.25, 0.05
kb_2	C	x	4.0, 1.0, 0.25, 0.05
	c.m.	x	1.0, 0.2, 0.05
	c.m.	xz	0.5, 0.05
	H	s	2.0, 0.5, 0.1
		x,z	1.0, 0.2, 0.05

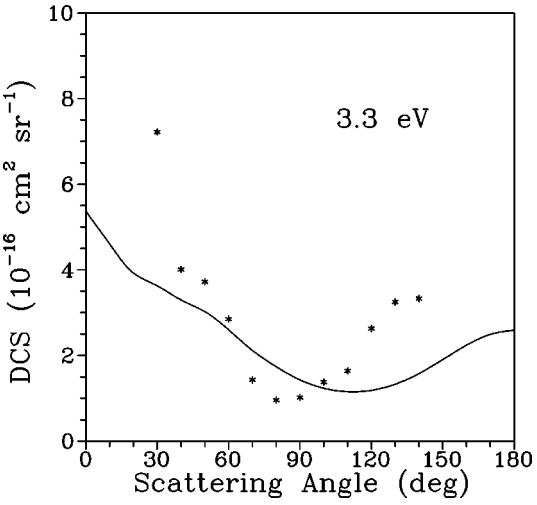

FIG. 1. DCS for elastic e^--C_2H_4 scattering at an impact energy of 3.3 eV. Solid line, present SECP results; asterisks, experimental results of Mapstone and Newell [3].

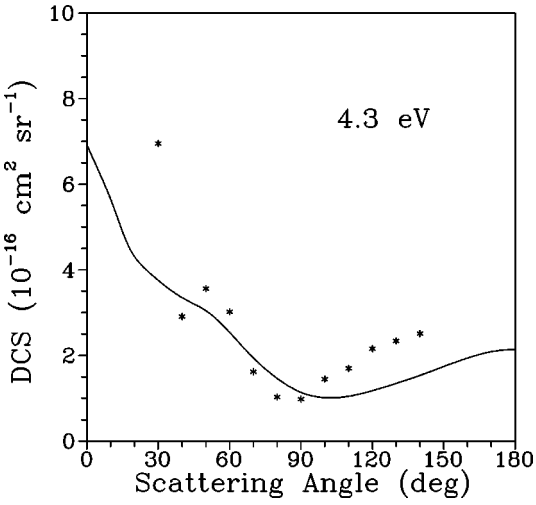

FIG. 2. Same as Fig. 1, but for 4.3 eV.

the free-particle wave vector $\Phi_{\vec{k}}^{(\pm)}$, a partial-wave on-shell T matrix (diagonal in both p and μ) is obtained:

$$T_{k,lh;l'h'}^{(\pm)p\mu}=\langle\Phi_{k,l'h'}^{(\mp)p\mu}|U|\tilde{\Psi}_{k,lh}^{(\pm)p\mu}\rangle+\langle\tilde{\Psi}_{k,l'h'}^{(\mp)p\mu}|U|\Phi_{k,lh}^{(\pm)p\mu}\rangle - \langle\tilde{\Psi}_{k,l'h'}^{(\mp)p\mu}|U-UG_0^{(\pm)}U|\tilde{\Psi}_{k,lh}^{(\pm)p\mu}\rangle, \tag{6}$$

where $k=|\vec{k}_0|=|\vec{k}|$ for the elastic process.

The initial scattering wave functions can be expanded in a set R_0 of L^2 basis functions $\alpha_i(\vec{r})=\langle\vec{r}|\alpha_i\rangle$:

$$\tilde{\Psi}_{k,lh}^{(\pm)p\mu}(\vec{r})=\sum_{i=1}^{N} a_{i,lh}^{(\pm)p\mu}(k)\alpha_i(\vec{r}). \tag{7}$$

Using Eqs. (6) and (7), variational $T_{k,lh;l'h'}^{(\pm)p\mu}$ matrix elements can be derived as

$$T_{k,lh;l'h'}^{(\pm)p\mu}=\sum_{i,j=1}^{N}\langle\Phi_{k,l'h'}^{(\mp)p\mu}|U|\alpha_i\rangle[D^{(\pm)^{-1}}]_{ij}\langle\alpha_j|U|\Phi_{k,lh}^{(\pm)p\mu}\rangle, \tag{8}$$

where

$$D_{ij}^{(\pm)}=\langle\alpha_i|U-UG_0^{(\pm)}U|\alpha_j\rangle \tag{9}$$

and the corresponding approximate scattering solution with outgoing-wave boundary condition becomes

$$\Psi_{k,lh}^{(+)p\mu^{(S_0)}}(\vec{r})=\Phi_{k,lh}^{p\mu}(\vec{r})+\sum_{i,j=1}^{M}\langle\vec{r}|G_0^{(+)}U|\alpha_i\rangle \times[D^{(+)^{-1}}]_{ij}\langle\alpha_j|U|\Phi_{k,lh}^{p\mu}\rangle. \tag{10}$$

Converged outgoing solutions of Eq. (2) can be obtained via an iterative procedure. The method consists in augmenting the basis set R_0 by the set

$$S_0=\{\Psi_{k,l_1h_1}^{(+)p\mu^{(S_0)}}(\vec{r}),\Psi_{k,l_2h_2}^{(+)p\mu^{(S_0)}}(\vec{r}),\ldots,\Psi_{k,l_ch_c}^{(+)p\mu^{(S_0)}}(\vec{r})\}, \tag{11}$$

TABLE III. Eigenphase sums (for the C_{2v} point group) in the iterative procedure.

Energy (eV)	Scattering symmetry	Iteration 0	1	2	3	4
0.1	ka_1	−0.0726	0.0561	0.0587	0.0582	0.0582
	ka_2	0.0003	0.00243	0.00244	0.00244	
	kb_1	−0.0027	−0.0174	−0.0171	−0.0171	
	kb_2	0.0205	0.0832	0.0832	0.0832	
1	ka_1	−0.333	−0.0968	−0.0930	−0.0938	−0.0936
	ka_2	0.0501	0.115	0.115	0.115	
	kb_1	0.0323	0.119	0.122	0.122	
	kb_2	0.229	0.388	0.388	0.388	
10	ka_1	2.500	3.680	3.713	3.700	3.690
	ka_2	1.143	1.601	1.603	1.600	
	kb_1	−1.337	−0.380	−0.383	−0.383	
	kb_2	0.975	1.737	1.742	1.742	

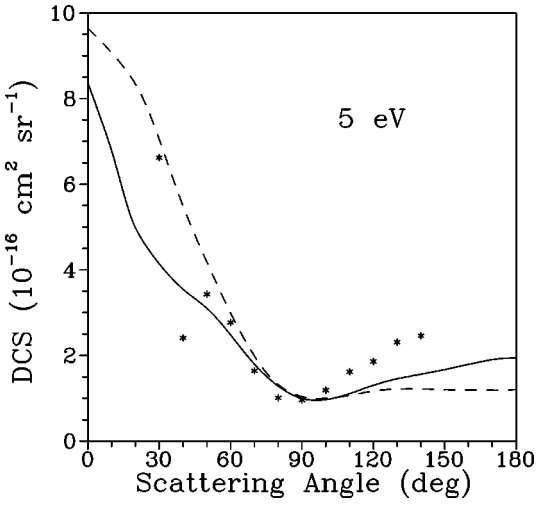

FIG. 3. DCS for elastic e^--C_2H_4 scattering at an impact energy of 5 eV. Solid line, present SECP results; dashed line, Schwinger multichannel (SE) calculated results of Winstead *et al.* [6]; asterisks, experimental results of Mapstone and Newell [3].

where l_c is the maximum value of l for which the expansion of the scattering solution (3) is truncated. A new set of partial-wave scattering solutions can now be obtained from

$$\Psi_{k,lh}^{(+)p\mu^{(S_1)}}(\vec{r}) = \Phi_{k,lh}^{p\mu}(\vec{r}) + \sum_{i,j=1}^{M} \langle \vec{r}|G^{(+)}U|\eta_i^{(S_0)}\rangle \times [D^{(+)^{-1}}]_{ij}\langle \eta_j^{(S_0)}|U|\Phi_{k,lh}^{p\mu}\rangle, \tag{12}$$

where $\eta_i^{(S_0)}(\vec{r})$ is any function in the set $R_1 = R_0 \cup S_0$ and M is the number of functions in R_1. This iterative procedure continues until a converged $\Psi_{k,lh}^{(+)p\mu^{(S_n)}}$ is achieved. These converged scattering wave functions correspond, in fact, to exact solutions of the truncated Lippmann-Schwinger equation with the potential U.

In an actual calculation we compute the converged partial-wave K-matrix elements $K_{k,lh;l'h'}^{p\mu^{(S_n)}}$. These K-matrix elements can be obtained by replacing $D^{(+)}$ by its principal

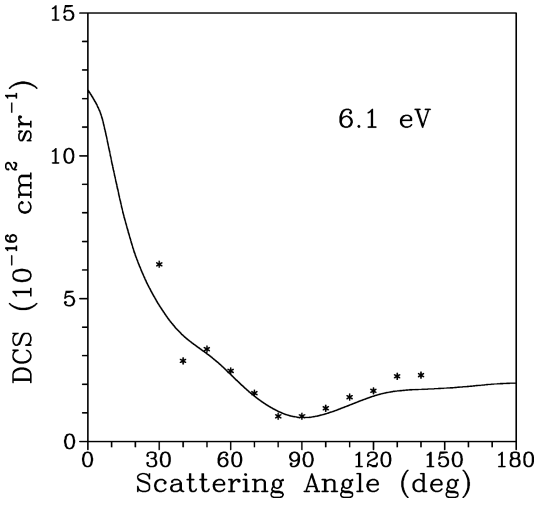

FIG. 4. Same as Fig. 1, but for 6.1 eV.

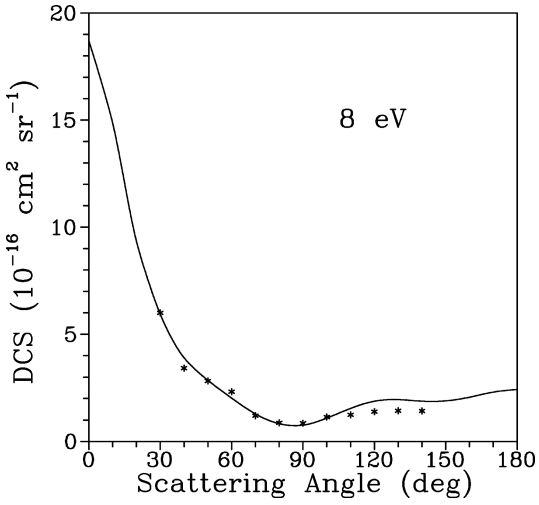

FIG. 5. Same as Fig. 1, but for 8 eV.

value $D^{(P)}$ in Eq. (8). Hence the corresponding partial-wave T-matrix elements can be calculated from

$$T_{k,lh,l'h'}^{p\mu^{(S_n)}} = -\left[\frac{2}{\pi}\right] \sum_{l'',h''} [1 - iK^{(S_n)}]_{k,lh;l''h''}^{p\mu} K_{k,l'',h'';l'h'}^{p\mu^{(S_n)}}. \tag{13}$$

By usual transformations, these matrix elements can be expressed in the laboratory frame (LF). The LF scattering amplitude $f(\hat{k}', \hat{k}_0')$ is related to the T matrix by

$$f(\hat{k}', \hat{k}_0') = -2\pi^2 T, \tag{14}$$

where $\hat{k}_0'$ and $\hat{k}'$ are the directions of incident and scattered electron linear momenta, respectively. The differential cross section for elastic electron-molecule scattering is given by

$$\frac{d\sigma}{d\Omega} = \frac{1}{8\pi^2} \int d\alpha \, (\sin\beta) d\beta \, d\gamma |f(\hat{k}', \hat{k}_0')|^2. \tag{15}$$

Here (α,β,γ) are the Euler angles that define the orientation of the principal axes of the molecule. Finally, after some

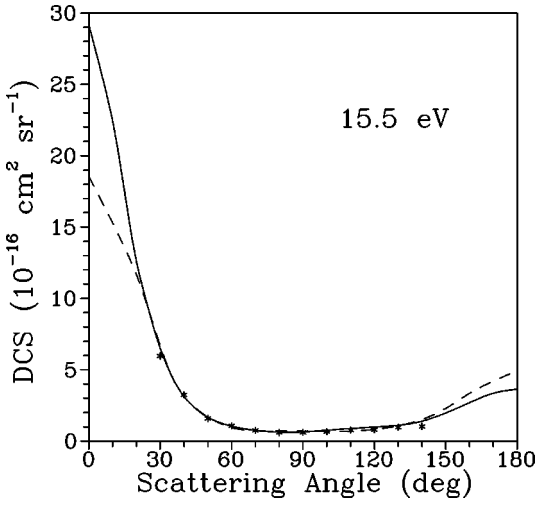

FIG. 6. Same as Fig. 3, but for 15.5 eV.

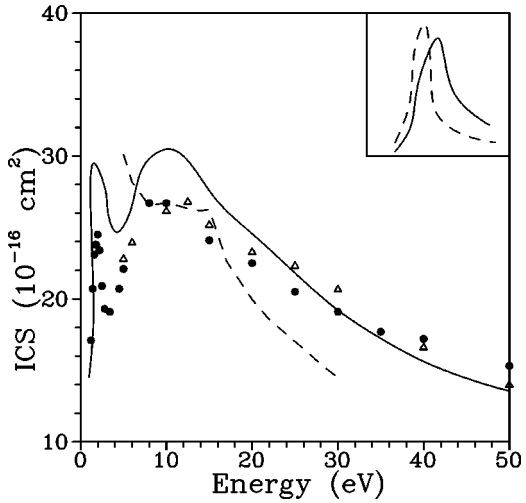

FIG. 7. ICS for e^--C_2H_4 scattering. Solid line, present SVIM results; dashed line, Schwinger multichannel (SE) results of Winstead *et al.* [6]; circles, experimental results of Sueoka and Mori [2]; triangles, experimental data of Floeder *et al.* [1]. Inset: partial ICS ($^2B_{2g}$ symmetry) in the (1.0–4.5)-eV range. Dashed line, Kohn variational results of Schneider *et al.* [5].

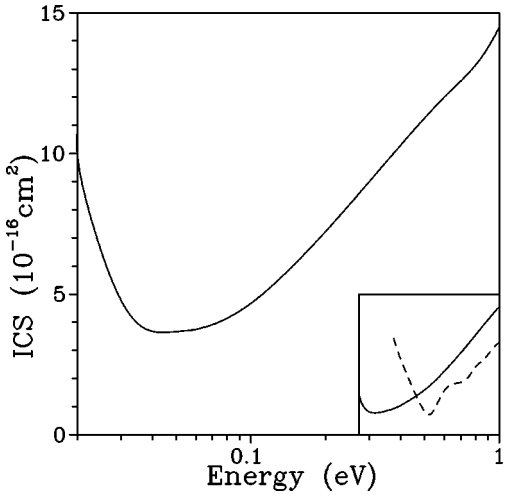

FIG. 8. Present SECP ICS for e^--C_2H_4 scattering below 1 eV. Inset: partial ICS (^2A_g symmetry). Solid line, present SVIM results; dashed line, Kohn variational results of Schneider *et al.* [5].

angular-momentum algebra, the LF DCSs averaged over the molecular orientations can be written as

$$\frac{d\sigma}{d\Omega}=\sum_L A_L(k)P_L(\cos\theta), \tag{16}$$

where θ is the scattering angle. The coefficients $A_L(k)$ in Eq. (16) are given by the formula

$$\begin{aligned}A_L(k)=&\frac{1}{2}\frac{1}{2L+1}\sum_{\substack{p,\mu,l,h,l',h',m,m'\\ p_1,\mu_1,l_1,h_1,l_1',h_1',m_1,m_1'}}\\ &\times(-1)^{m'-m}\sqrt{(2l+1)(2l_1+1)}\\ &\times b^{p_1\mu_1}_{l_1'h_1'm_1'}b^{p_1\mu_1*}_{l_1h_1m_1}b^{p\mu*}_{l'h'm'}b^{p\mu}_{lhm}a^{p_1\mu_1^*}_{l_1h_1,l_1'h_1'}(k)a^{p\mu}_{lh,l'h'}(k)\\ &\times(l_10l0|L0)(l_1'0l'0|L0)(l_1-m_1lm|L-M)\\ &\times(l_1'm_1'l'm'|LM),\end{aligned} \tag{17}$$

where $(j_1m_1j_2m_2|j_3m_3)$ are the usual Clebsch-Gordan coefficients and the auxiliary amplitudes $a^{p\mu}_{lh,l'h'}(k)$ are defined as

$$a^{p\mu}_{lh,l'h'}(k)=-\frac{\sqrt{\pi^3}}{k}i^{l'-l}\sqrt{2l'+1}T^{p\mu^{(S_n)}}_{k,lh;l'h'}. \tag{18}$$

The self-consistent-field (SCF) wave function for the ground state used in the static-exchange calculation was obtained using the contracted Gaussian basis set shown in Table I. It consists of the contracted set of Dunning [15] augmented with some uncontracted functions on the nuclei and on the center of mass of the molecule. At the experimental equilibrium geometry of $R_{(C—C)}=2.5133$ a.u., $R_{(C—H)}=2.0333$ a.u., and $\theta_{(H—C—H)}=116.6°$, this basis set gives a SCF energy of -78.06060 a.u. This value compares well with the near-Hartree-Fock limit of -78.0616 a.u. [16]. The resulting orbital energies are $-11.230\,09$, $-11.228\,35$, $-1.036\,66$, $-0.796\,66$, $-0.646\,01$, $-0.591\,76$, $-0.509\,54$, and $-0.377\,02$ a.u. for the $1a_g$, $1b_{1u}$, $2a_g$, $2b_{1u}$, $1b_{2u}$, $3a_g$, $1b_{3g}$, and $1b_{3u}$ orbitals, respectively. The correlation-polarization effects are introduced in the potential through a parameter-free model that combines the target correlation calculated from the local electron-gas theory for short distances with the asymptotic form of the polarization potential [13]. The dipole polarizabilities used in the calculation of the correction to the SE potential are derived from the experimental values published in Ref. [17]: $\alpha_{00}=28.4667$, $\alpha_{20}=7.923$, and $\alpha_{22}=0.2625$. All partial-wave expansions were truncated at $l_c=12$ and $l_c=16$ for incident energies below and above 20 eV, respectively, and all possible values of $h\leqslant l$ were retained. The resulting orbital normalizations were better than 0.999 for all bound orbitals.

The discussion of the convergence in the iterative procedure is interesting in itself. As discussed above, this procedure starts with trial scattering functions represented by a basis set R_0. The R_0 used in the present calculation is shown in Table II. The convergence rate of the iterative procedure can be demonstrated, for example, by the evolution of the eigenphase sums. This evolution is shown in Table III for each IR of the C_{2v} point group and for three selected energies (0.1, 1.0, and 10 eV). Similar convergence rates are also seen for the other incident energies studied herein. As it can be seen from that table, our SVIM calculations were all converged within four iterations.

III. RESULTS AND DISCUSSION

We have selected representative results on DCSs, mostly where experimental data and/or other calculations are available for comparison. The calculated DCSs for e^--C_2H_4 scattering at incident energies $E_0=3.3$, 4.3, 5, 6.1, 8, and 15.5 eV are shown in Figs. 1–6, along with the experimental results of Mapstone and Newell [3]. Theoretical cross sections of Winstead *et al.* [6] are also included at 5 and 15 eV. The measured data of Mapstone and Newell are relative.

TABLE IV. DCSs, ICSs, and MTCSs (in 10^{-16} cm^2) for elastic e^--C_2H_4 scattering.

Angle (deg)	E_0 (eV)								
1	3.3	4.3	5	6.1	8	15.5	30	50	
0	1.69	5.38	6.92	8.36	12.31	18.68	29.13	33.55	38.82
10	1.24	4.60	5.65	6.78	9.79	14.85	22.41	23.04	21.11
20	0.70	3.92	4.31	4.98	6.51	9.34	12.59	9.97	6.67
30	0.55	3.63	3.76	4.14	4.76	5.94	6.51	4.04	2.28
40	0.58	3.30	3.35	3.55	3.71	3.90	3.12	1.64	1.12
50	0.85	3.03	3.05	3.10	3.07	2.85	1.67	0.94	0.62
60	1.14	2.60	2.54	2.48	2.34	2.02	1.05	0.65	0.42
70	1.35	2.12	1.94	1.80	1.59	1.28	0.76	0.54	0.36
80	1.52	1.74	1.46	1.28	1.05	0.83	0.63	0.49	0.33
90	1.57	1.43	1.14	1.00	0.83	0.76	0.64	0.50	0.32
100	1.51	1.23	1.01	0.97	0.97	1.09	0.76	0.51	0.30
110	1.40	1.16	1.05	1.11	1.27	1.54	0.88	0.55	0.31
120	1.24	1.18	1.18	1.30	1.58	1.88	0.99	0.61	0.35
130	1.06	1.33	1.35	1.46	1.77	1.95	1.11	0.72	0.41
140	0.92	1.58	1.53	1.56	1.82	1.88	1.40	0.85	0.48
150	0.91	1.90	1.74	1.67	1.86	1.89	2.00	0.98	0.54
160	0.73	2.24	1.94	1.79	1.93	2.06	2.69	1.13	0.60
170	0.69	2.49	2.09	1.90	2.00	2.30	3.36	1.26	0.67
180	0.68	2.59	2.14	1.95	2.04	2.42	3.63	1.33	0.70
ICS	14.52	25.67	24.65	25.10	27.01	29.80	27.17	19.24	13.56
MTCS	14.86	20.87	19.17	18.96	20.17	21.18	16.32	9.49	5.52

However, at 8 and 15.5 eV their results have been normalized to the theoretical calculations of McKoy [18] at 7.5 and 15 eV, respectively. In this work, the comparison shown in Figs. 1–6 is made by using directly the results published in Table III of Mapstone and Newell's work. Although no further normalization has been introduced for this comparison, there is good agreement between our calculations and the experimental results, particularly for incident energies above 5 eV. In the (3.3–6.1)-eV energy range, the measured DCSs show a pronounced minimum at 90° and a much smaller dip centered around 40° followed by a local maximum around 65°. According to Mapstone and Newell, these structures display characteristics associated with an f-wave resonance. Such structures are not seen in our calculated DCSs in this energy region, although some evidence of their occurrence can be seen in our data. Indeed, a partial-wave analysis has shown the existence of an f-wave resonance in the B_{1u} scattering channel centered at around 10 eV. This resonance is responsible for the enhancement of the ICSs in this energy region and is in accordance with the measured total cross sections of Floeder *et al.* [1] and of Sueoka and Mori [2], as we will see in Fig. 7. The comparison with the SE calculated cross sections of Winstead *et al.* [6] shows that the polarization potential has little effect on the qualitative behavior of the DCSs. Also, the influence of the correlation-polarization potential is small for backward scattering; it manifests mainly in the forward direction especially for low incident energies.

In Fig. 7 the calculated ICSs in the (1–50)-eV energy range are presented, as a function of the incident energy, along with the experimental results of Floeder *et al.* [1] and of Sueoka and Mori [2] and the theoretical SE results of Winstead *et al.* [6]. The inset of this figure shows a qualitative comparison of our partial ICSs for the $^2B_{2g}$ symmetry in the (1.0–4.5)-eV range with the calculated data of Schneider *et al.* [5]. Two structures characterize the ICS curve for e^--ethylene collisions: a sharp peak at approximately 2.5 eV and, similarly to CH_4, a broad peak centered around 10 eV in our calculations. As shown in the inset, the first structure is a shape resonance in the $^2B_{2g}$ symmetry, which corresponds to a temporary capture of the incident electron into an antibonding valence orbital. In general, our static exchange-correlation polarization (SECP) ICSs are in good agreement with the measured data, particularly for incident energies $E_0 \geqslant 15$ eV, although at lower energies our calculations tend to overestimate the ICSs. The SE results show qualitative disagreement with our results and also deviate from experiment at higher energies.

It is interesting to note the behavior of the ICSs in the low-energy region (below 1 eV). The scattering in this region is dominated by the totally symmetric ^2A_g scattering channel, which is largely affected by the dipolar distortion of the charge cloud of the target by the incident electron. Our SECP results of ICSs below 1.0 eV are shown in Fig. 8. The results for ^2A_g partial ICSs in the same energy range are shown in the inset, where the theoretical results of Schneider *et al.* [5] are also included for qualitative comparison. Our calculated ICSs show a well-pronounced minimum around 0.05 eV, which is associated with the Ramsauer-Townsend (RT) minimum. This finding supports the evidence for the existence of such minimum at very low energies provided by two experimental works: The data from Swarm experiments carried out by Boness *et al.* [19] show a maximum in the transmission function for electrons through the ethylene gas

at approximately 200 meV; Hayashi's work [20] presents a minimum in the momentum-transfer cross sections near 100 meV. Also, theoretically, a minimum in the partial ^2A_g ICSs was recently predicted by the calculations of Schneider *et al.* [5], although slightly shifted from our results (see the inset). The RT minimum is also present in other molecules, although calculations at the SE level of approximation are not able to reproduce it. For the sake of completeness, in Table IV we also present our calculated DCSs, ICSs, and MTCSs for energies ranging from 1 to 50 eV.

IV. CONCLUSIONS

We have reported the results of DCSs, ICSs, and MTCSs for e^--C_2H_4 scattering. This calculation of DCSs for this molecule includes polarization effects. We have observed a shape resonance in the ICSs at around 2.5 eV in good agreement with available experimental data; our model was also able to reproduce the RT minimum in the ICSs at very low energies, in qualitative agreement with previous experimental and theoretical predictions. With the recent extension of our SECP numerical codes in order to study electron scattering by nonplanar molecules possessing symmetries reducible to C_{2v}, calculations of cross sections for other systems (such as SiH_4 and GeH_4) are under way.

ACKNOWLEDGMENTS

This research was partially supported by the National Science Foundation, the Conselho Nacional de Desenvolvimento Científico e Tecnológico (CNPq), FINEP-PADCT, CAPES-PADCT, and FAPESP.

[1] K. Floeder, D. Fromme, W. Raith, A. Schwab, and G. Sinapius, J. Phys. B **18**, 3347 (1985).
[2] O. Sueoka and S. Mori, J. Phys. B **19**, 4035 (1986).
[3] B. Mapstone and W. R. Newell, J. Phys. B **25**, 491 (1992).
[4] S. L. Lunt, J. Randell, J. P. Ziesel, G. Mrotzek, and D. Field, J. Phys. B **27**, 1407 (1994).
[5] B. I. Schneider, T. N. Rescigno, B. H. Lengsfield III, and C. W. McCurdy, Phys. Rev. Lett. **66**, 2728 (1991).
[6] C. Winstead, P. G. Hipes, M. A. P. Lima, and V. McKoy, J. Chem. Phys. **94**, 5455 (1991).
[7] L. E. Machado, M.-T. Lee, and L. M. Brescansin (unpublished).
[8] R. R. Lucchese, G. Raseev, and V. McKoy, Phys. Rev. A **25**, 2572 (1982).
[9] L. E. Machado, L. M. Brescansin, M. A. P. Lima, M. Braunstein, and V. McKoy, J. Chem. Phys. **92**, 2362 (1990).
[10] L. E. Machado, E. P. Leal, M.-T. Lee, and L. M. Brescansin, J. Mol. Struct. **335**, 37 (1995).
[11] L. E. Machado, M.-T. Lee, L. M. Brescansin, and M. A. P. Lima, J. Phys. B **28**, 467 (1995).
[12] L. M. Brescansin, M.-T. Lee, L. E. Machado, M. A. P. Lima, and V. McKoy (unpublished).
[13] N. T. Padial and D. W. Norcross, Phys. Rev. A **29**, 1742 (1984).
[14] P. G. Burke, N. Chandra, and G. N. Thompson, J. Phys. B **5**, 2212 (1972).
[15] T. H. Dunning, Jr., J. Chem. Phys. **53**, 2823 (1970).
[16] E. Clementi and H. Popkic, J. Chem. Phys. **57**, 4870 (1972).
[17] G. W. Hills and W. J. Jones, J. Chem. Soc. Faraday Trans. II **71**, 812 1975.
[18] V. McKoy, as cited in Ref. [3].
[19] M. J. W. Boness, I. W. Larkin, J. B. Hasted, and L. Moore, Chem. Phys. Lett. **1**, 292 (1967).
[20] M. Hayashi, in *Non-Equilibrium Processes in Partially Ionized Gases*, edited by M. Capitelli and J. N. Bardsley (Plenum, New York, 1990), p. 333.